Alumination and Ion Exchange of Mesoporous SBA-15 Molecular Sieves

Zhaohua Luan,[†] Martin Hartmann,[‡] Dongyuan Zhao,[§] Wuzong Zhou,[∥] and Larry Kevan*,[†]

Department of Chemistry, University of Houston, Houston, Texas 77204-5641, Institut für Technische Chemie I, Universität Stuttgart, D-70550 Stuttgart, Germany, Department of Chemistry, Fudan University, Shanghai, 200433, China, and Department of Chemistry, University of Cambridge, Lensfield Road, Cambridge CB2 1EW, U.K.

Received February 4, 1999. Revised Manuscript Received April 16, 1999

Mesoporous silica SBA-15 molecular sieve has been synthesized and incorporated with aluminum via three different postsynthesis procedures by reacting SBA-15 with $AlCl_3$ in dry ethanol (route 1), with aluminum isopropoxide in dry hexane (route 2) and with an aqueous solution of sodium aluminate (route 3) followed by calcination. Characterization by transmission electron microscopy, N_2 adsorption, electron probe microanalysis, powder X-ray diffraction, ^{27}Al magic-angle-spinning NMR, and electron spin resonance spectroscopies has been carried out to evaluate the efficiency of these alumination methods and their effect on the pore structure and ion exchange capacity of SBA-15. The Si/Al ratios in the resulting materials are in close agreement with the composition in the postsynthesis mixtures over a range of 40−10, indicating that the aluminum is mostly incorporated into silica SBA-15. The silanol groups on the internal wall surfaces of SBA-15 are suggested to be the sites for aluminum incorporation. The incorporation procedure has a strong effect on the aluminum coordination, pore structure and ion exchange capacity of the resulting materials. At comparable Si/Al ratios around 20, the percentage of aluminum with tetrahedral symmetry in the synthesized materials is about 100% (route 3) > 76% (route 1) > 71% (route 2), indicating that alumination by aqueous sodium aluminate is most effective. This is probably due to the presence of Na^+ ions which balance the negative charges associated with tetrahedral aluminums. The BET specific surface areas are 85% (route 1) > 60% (route 2) > 42%(route 3), showing that alumination by $AlCl_3$ in ethanol best maintains the mesoporous structure of SBA-15. Electron-spin resonance reveals a linear dependence of the Cu(II) ion exchange capacity on the tetrahedral aluminum content of the aluminum-containing SBA-15 materials. This suggests that the incorporated aluminums in the tetrahedral framework do serve as ion exchange sites.

Introduction

Microporous aluminosilicate molecular sieves known as zeolites contain regular arrays of uniformly sized channels and admit molecules below a certain critical size into their internal space which makes them useful as heterogeneous catalysts and sorbents.[1] Processing large organic molecules as in fine chemical production often requires a molecular sieve with a larger pore size than the 15 Å or less of conventional zeolites. This is satisfied by tubular aluminosilicate MCM-41 materials which possess uniform mesopore channels varying from about 15 Å to 100 Å with a large internal surface area up to 1000 m^2/g.[2] A recently discovered silica phase, designated as SBA-15, further expands the channels for such materials to the macroporous regime up to 300 Å.[3]

Ion-exchange, catalytic and adsorptive properties of molecular sieve materials originate from acid sites which arise from the presence of accessible hydroxyl groups associated with tetrahedral framework aluminum in a silica matrix.[4,5] Purely siliceous molecular sieve materials have an electrically neutral framework and consequently no acid sites. Much effort has therefore been devoted to the introduction of aluminum into silica frameworks.[4−8] Typically, aluminum is incorporated into the framework of a silicate material via a so-

[†] University of Houston.
[‡] Universität Stuttgart.
[§] Fudan University.
[∥] University of Cambridge.

(1) Bellussi, G.; Rigutto, M. S. In *Advanced Zeolite Science and Applications*; Jansen, J. C., Stöcker, M., Karge, H. G., Weitkamp, J., Eds.; Studies in Surface Science and Catalysis; Elsevier: Amsterdam, 1994; Vol. 85, 177−213.
(2) Kresge, C. T.; Leonowicz, M. E.; Roth, W. J.; Vartuli, J. C.; Beck, J. S. *Nature* **1992**, *359*, 710.
(3) Zhao, D.; Feng, J.; Huo, Q.; Melosh, N.; Fredrickson, G. H.; Chmelka, B. F.; Stucky, G. D. *Science* **1998**, *279*, 548.
(4) Corma, A.; Fornés, V.; Navarro, M. T.; Pérez-Pariente, J. *J. Catal.* **1994**, *148*, 569.
(5) Luca, V.; MacLachlan, D. J.; Bramley, R.; Morgan, K. *J. Phys. Chem.* **1996**, *100*, 1793.
(6) Chen, C.-Y.; Li, H.-X.; Davis, M. E. *Microporous Mater.* **1993**, *2*, 17.
(7) Schmidt, R.; Akporiaye, D.; Stöcker, M.; Ellestad, O. H. *J. Chem. Soc., Chem. Commun.* **1994**, 1493.
(8) Luan, Z.; He, H.; Cheng, C.-F.; Zhou, W.; Klinowski, J. *J. Phys. Chem.* **1995**, *99*, 1018.

10.1021/cm9900756 CCC: $18.00
Published on Web 05/13/1999

called "direct synthesis" procedure in which an aluminum precursor is added into the gel prior to hydrothermal synthesis. This direct synthesis method often requires specialized synthesis conditions depending on the respective structures of the materials, and the incorporation of aluminum into the silica matrix usually causes a decrease in the structural ordering.[8]

SBA-15 is a purely siliceous phase synthesized in strong acidic media (2 M HCl solution).[3] Since most aluminum sources dissolve in strong acids, precipitation to incorporate framework aluminum into SBA-15 by direct synthesis seems unlikely. Previous studies have shown that aluminum can be effectively incorporated into siliceous MCM-41 materials via various postsynthesis procedures by grafting aluminum onto MCM-41 wall surfaces with anhydrous $AlCl_3$[9] or aluminum isopropoxide in nonaqueous solution,[10] or with sodium aluminate in aqueous solution[11] followed by calcination. The authors claimed that the materials produced via these postsynthesis procedures have superior structural integrity, acidity and catalytic activity to those of materials having aluminum incorporated during synthesis.

In this work mesoporous siliceous SAB-15 molecular sieve has been synthesized and then varying amounts of framework aluminum have been incorporated via three postsynthesis procedures. The efficiency of these postsynthesis methods for aluminum incorporation and their effect on the pore structure and ion exchange capacity of siliceous SBA-15 have been evaluated by a combination of characterization techniques including transmission electron microscopy (TEM), N_2 adsorption, electron probe microanalysis (EPMA), powder X-ray diffraction (XRD), ^{27}Al magic-angle-spinning (MAS) NMR, and electron spin resonance (ESR) spectroscopies.

Experimental Section

Samples. A detailed synthesis procedure for mesoporous silica SBA-15 has been reported.[3] In a typical synthesis in this work, 2 g of amphiphilic triblock copolymer, poly(ethylene glycol)-*block*-poly(propylene glycol)-*block*-poly(ethylene glycol) (average molecular weight 5800, Aldrich), was dispersed in 15 g of water and 60 g of 2 M HCl solution while stirring, followed by the addition of 4.25 g of tetraethyl orthosilicate (Aldrich) to the homogeneous solution with stirring. This gel mixture was continuously stirred at 40 °C for 24 h, and finally crystallized in a Teflon-lined autoclave at 100 °C for 2 days. After crystallization the solid product was centrifuged, filtered, washed with deionized water, and dried in air at room temperature. The material was calcined in static air at 550 °C for 24 h to decompose the triblock copolymer and obtain a white powder (SBA-15). This white powder is used as the parent material to produce aluminum-containing materials, AlSBA-15, via three different postsynthesis routes.

Route I.[9] Silica SBA-15 (0.5 g) was combined with 50 mL of dry ethanol containing various amounts of $AlCl_3$ with magnetic stirring at room temperature for 12 h. The solid material was then filtered, washed vigorously with dry ethanol, and dried at room temperature in air.

Route II.[10] Silica SBA-15 (0.5 g) was dispersed in 50 mL of dry hexane containing various amounts of aluminum isopropoxide. The resulting mixture was stirred at room temperature for 12 h, and the powder was filtered, washed with dry hexane, and dried at room temperature in air.

Route III.[11] Alumination was conducted by stirring 0.5 g of silica SBA-15 in 50 mL of water containing various amounts of sodium aluminate at room temperature for 12 h. The solid material was then filtered, washed with distilled water, and dried at room temperature in air.

These three solid powders were calcined in static air at 550 °C for 5 h. These materials are designated as I-, II-, or III-AlSBA-15-(X), where X is the Si/Al ratio from the chemical stoichiometric composition in the postsynthesis mixtures.

To evaluate the ion exchange capacity, Cu(II) was ion-exchanged into SBA-15 and AlSBA-15 materials by stirring a powder sample in a 20 times by weight solution of 1 N $CuSO_4$ for 1 h at about 95 °C. The resultant solid was then filtered and washed with hot distilled water to remove physically adhered Cu(II) ions.

Characterization. The elemental composition of the resultant solid products was analyzed by a JEOL JXA-8600 Electron Beam Superprobe operated at a beam voltage of 15 kV and current of 30 nA. Si and O were calibrated with diopsite, $CaMgSi_2O_6$, Cu with Cu_2O, and Al with anorthite, $CaAl_2Si_2O_8$. The X-ray yields from these standards and samples were measured using a wavelength dispersive spectrometer. Prior to measurement, the samples were prepared as pressed pellets to make a dense material with a reasonably smooth surface. The electron beam was defocused to 10 μm diameter to minimize the damage caused to the specimen by heating. Data were collected from 3 to 5 randomly chosen regions and averaged to represent the bulk composition. No significant differences were seen between the regions which indicates a uniform elemental composition over the sample. The precision was <1% for all elements and the accuracy is estimated at ±2−3% for cations and ±5% for oxygen.

Powder XRD patterns were collected before and after calcination using a Scintag PADX diffractometer equipped with a liquid nitrogen cooled germanium solid-state detector using Cu Kα radiation. For TEM, calcined specimens of SBA-15 were ground and dried in an oven at 550 °C for 1 h. After being cooled to room temperature in a vacuum, the dried powder was deposited on a grid of holey carbon film and rapidly transferred to a JEM-200CX electron microscope operating at 200 kV.

N_2 adsorption isotherms were measured at 77 K using a Micromeritics Gemini 2375 analyzer. The volume of adsorbed N_2 was normalized to standard temperature and pressure. Prior to the experiments, samples were dehydrated at 250 °C for 5 h. The specific surface area, A_{BET}, was determined from the linear part of the BET equation ($P/P_0 = 0.05-0.31$). The calculation of the mesopore size distribution was performed using the desorption branches of the N_2 adsorption isotherms and the Barrett−Joyner−Halenda (BJH) formula.[12] The mesopore surface area, A_{BJH}, volume, V_{BJH}, and pore diameter, D_{BJH}, were obtained from the pore size distribution curves.

^{27}Al MAS NMR spectra were recorded at 9.4 T using a Bruker MSL 400 spectrometer with a 4-mm-diameter rotor spun at 9 kHz. Spectra were measured at 104.26 MHz with a recycle delay of 0.5 s. All samples were fully hydrated prior to measurement,[13] and short $\pi/20$ radio frequency pulses were used so that the ^{27}Al spectra should be quantitatively comparable.[14] External $Al(H_2O)_6^{3+}$ was used as a reference.

For ESR, samples were loaded into 3 mm o.d. by 2 mm i.d. Suprasil quartz tubes. ESR spectra were recorded at X-band at either 293 or 77 K on a Bruker ESP 300 spectrometer. The Bruker ESP 300E software was used for double integration of the signal intensity. The magnetic field was calibrated with a Varian E−500 gaussmeter. The microwave frequency was measured by a Hewlett-Packard HP 5342A frequency counter.

(9) Ryoo, R.; Jun, S.; Kim, J. M.; Kim, M. J. *Chem. Commun.* **1997**, 2225.
(10) Mokaya, R.; Jones, W. *Chem. Commun.* **1997**, 2185.
(11) Hamdan, H.; Endud, S.; He, H.; Muhid, M. N. M.; Klinowski, J. *J. Chem. Soc., Faraday Trans.* **1996**, *92*, 2311.
(12) Barrett, E. P.; Joyner, L. G.; Halenda, P. P. *J. Am. Chem. Soc.* **1951**, *73*, 373.
(13) Ray, G. J.; Meyers, B. L.; Marshall, C. L. *Zeolites* **1987**, *7*, 307.
(14) Man, P. P.; Klinowski, J.; Trokiner, A.; Zanni, H.; Papon, P. *Chem. Phys. Lett.* **1988**, *151*, 143.

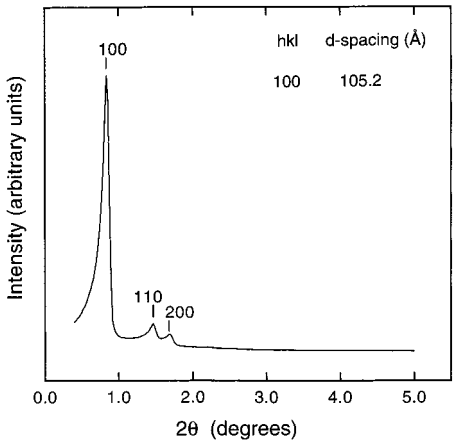

Figure 1. XRD pattern of siliceous SBA-15 molecular sieve.

Results

XRD. Small-angle XRD of siliceous SBA-15 is shown in Figure 1. This very low angle data was collected by Dr. Zhao on special instrumentation at the University of California, Santa Barbara. It shows a well-resolved pattern with a prominent peak at 0.8°, and two weak peaks at 1.6 and 1.7° 2θ, which match well with the pattern reported for SBA-15.[3] This confirms successful synthesis of SBA-15 silica. The XRD peaks can be indexed to a hexagonal lattice with a $d(100)$ spacing of 105 Å, corresponding to a large unit cell parameter a_0 = 122 Å ($a_0 = 2d(100)/\sqrt{3}$). In contrast with MCM-41 which shows significant unit cell contraction after calcination,[8] calcination of SBA-15 does not affect its XRD pattern except for increasing the signal intensity.

XRD patterns of AlSBA-15 with aluminum were not obtained since such low angle data cannot be obtained with our XRD instrumentation. Reliable information about the effect of aluminum incorporation on the pore structure of SBA-15 has been obtained from N_2 adsorption experiments as shown below.

TEM. Figure 2 shows the TEM images of siliceous SBA-15. The hexagonal array of uniform channels of ~60 Å in diameter is directly visible. However, as compared to previously reported TEM images for MCM-41 materials,[2,8] the TEM images from SBA-15 show much thicker walls of ~40 Å, which is consistent with the results from XRD and N_2 adsorption experiments (see below).

EPMA. EPMA analysis shows that all AlSBA-15 materials have a unique composition, therefore, the formation of Al_2O_3 can be excluded. The bulk Si/Al molar ratios listed in Table 1 are close to the values calculated from the initial postsynthesis mixtures except for higher concentrations by route I. This indicates that the aluminum has been mostly incorporated into the siliceous SBA-15.

Table 1 also lists the Cu/Al ratios of Cu(II) ion exchanged AlSBA-15 materials by EPMA. These show that the Cu(II) ion concentration corresponds to about 30% of the aluminums.

N_2 Adsorption. Figure 3 shows N_2 adsorption isotherm for siliceous SBA-15. A typical irreversible type IV adsorption isotherm with a H1 hysteresis loop, as defined by IUPAC,[15] is observed. The isotherm exhibits a sharp inflection in P/P_0 range from 0.60 to 0.80 characteristic of capillary condensation within uniform pores. The P/P_0 position of the inflection points is clearly related to a diameter in the mesopore range and the sharpness of the step indicates the uniformity of the mesopore size distribution. The pore size distribution can be calculated from the Kelvin equation[16,17] and is presented as a BJH plot in Figure 3 as an insert. It shows a very narrow pore size distribution with an

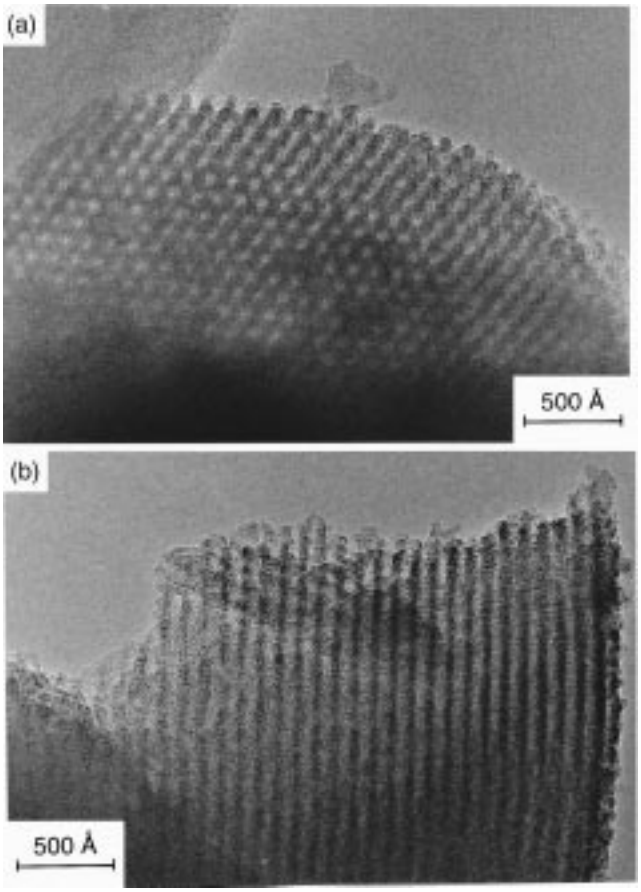

Figure 2. TEM images of siliceous SBA-15 (a) in the direction of the pore axis and (b) in the direction perpendicular to the pore axis.

Table 1. Elemental Composition and Aluminum Distribution of Mesoporous AlSBA-15 Molecular Sieves

	bulk			
samples	(Si/Al)[a]	Cu/Al[a]	Al(tet)/ (Al(tet)+Al(oct))[b]	framework (Si/Al)(tet)
I-AlSBA-15-(40)	40.0	0.32	0.77	51.9
I-AlSBA-15-(20)	33.3	0.20	0.76	43.8
I-AlSBA-15-(20)[c]	33.3	–	0.59	56.4
I-AlSBA-15-(10)	21.3	0.28	0.71	30.0
II-AlSBA-15-(40)	37.0	–	0.83	44.6
II-AlSBA-15-(20)	17.0	–	0.71	23.9
II-AlSBA-15-(20)[c]	17.0	–	0.72	23.6
II-AlSBA-15-(10)	8.5	–	0.61	13.9
III-AlSBA-15-(20)	20.8	0.33	1.00	20.8
III-AlSBA-15-(20)[c]	20.8	–	0.84	24.8

[a] By electron probe microanalysis. [b] Calculated from ^{27}Al MAS NMR spectra assuming that the relative content of aluminum is proportional to the intensity of the ^{27}Al MAS NMR lines. [c] Sample before calcination.

(15) Sing, K. S. W.; Everett, D. H.; Haul, R. A. W.; Moscow, L.; Pierotti, R. A.; Rouquerol, J.; Siemieniewska, T. *Pure Appl. Chem.* **1985**, *57*, 603.
(16) Tanev, P. T.; Vlaev. L. T. *J. Colloid Interface Sci.* **1993**, *160*, 110.
(17) Luan, Z.; He, H.; Zhou, W.; Cheng, C. F.; Klinowski, J. *J. Chem. Soc., Faraday Trans.* **1995**, *91*, 2955.

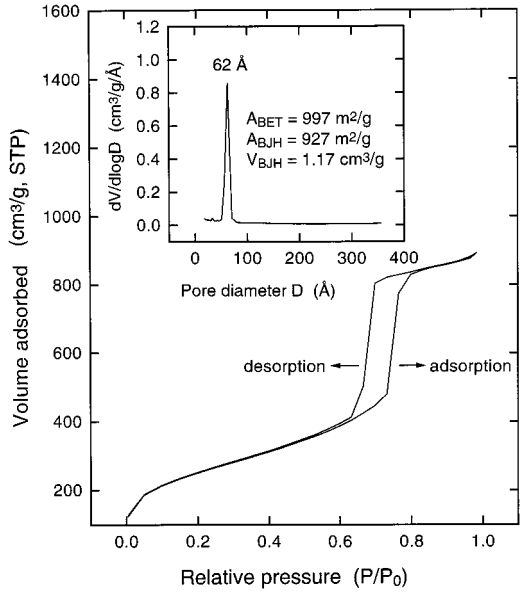

Figure 3. Adsorption−desorption isotherm of nitrogen on siliceous SBA-15 at 77 K. The insert shows the BJH pore size distribution calculated from the desorption branch of the isotherm.

Table 2. Pore Structure Parameters of AlSBA-15 Calculated from the Desorption Branch of Nitrogen Adsorption Isotherms Using the Barrett−Joyner−Halenda Formula

samples	A_{BJH} (m^2g^{-1})	V_{BJH} (cm^3g^{-1})	D_{BJH} (Å)	A_{BET} (m^2g^{-1})	ΔA_{BET} (%)
SBA-15	927	1.17	62.0	997	100
I-AlSBA-15-(40)	1041	1.43	62.1	1025	100
I-AlSBA-15-(20)	831	1.15	62.3	856	84
I-AlSBA-15-(10)	893	1.26	61.4	874	85
II-AlSBA-15-(40)	755	0.97	60.2	674	66
II-AlSBA-15-(20)	683	0.93	59.1	619	60
II-AlSBA-15-(10)	609	0.85	57.8	554	54
III-AlSBA-15-(20)	515	0.71	55.1	428	42

average mesopore size of 62 Å and a high surface area A_{BJH} of 927 m^2/g.

N_2 adsorption isotherms from all AlSBA-15 materials are quite similar to that from SBA-15 (not shown), while the inflection positions slightly shift toward lower P/P_0 values and the overall N_2 adsorption amounts decrease depending on the specific postsynthesis procedure and the aluminum loading. The calculated BET specific surface areas and mesopore parameters based on BJH plots are listed in Table 2. Alumination by reacting SBA-15 with $AlCl_3$ in dry ethanol (route 1) does not affect the original pore structure of the parent SBA-15 when the aluminum loading is low (I-AlSBA-15-(40)), while the surface areas slightly decrease as the aluminum loading increases (I-AlSBA-15-(20), I-AlSBA-15-(10)). In contrast, alumination by reacting SBA-15 with aluminum isopropoxide solution in dry hexane (route 2) or with an aqueous solution of sodium aluminate (route 3) reduce the surface area and narrow the pore diameter of the parent SBA-15. For III-AlSBA-15-(20) the BET specific surface area is only 42% of the parent SBA-15.

^{27}Al MAS NMR. Figure 4 shows the ^{27}Al MAS NMR spectra of I-AlSBA-15 produced by reacting siliceous SBA-15 with $AlCl_3$ in dry ethanol (route 1). All spectra give two resolved lines at 53 and 0 ppm. The line at 53 ppm can be assigned to aluminum in a tetrahedral environment (AlO_4 structural unit, Al(tet)), in which

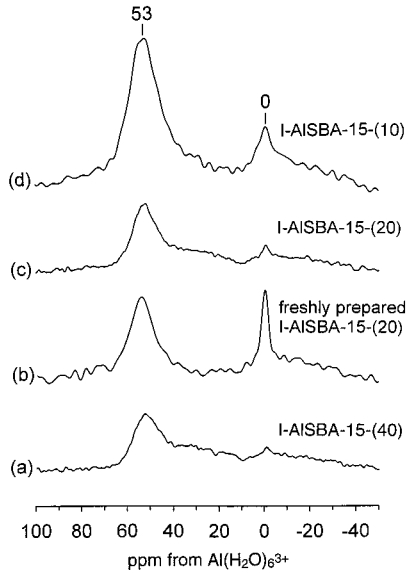

Figure 4. ^{27}Al MAS NMR spectra of calcined AlSBA-15 prepared by postsynthesis of SBA-15 with $AlCl_3$ in dry ethanol: (a) I-AlSBA-15-(40), (b) freshly prepared I-AlSBA-15-(20), (c) I-AlSBA-15-(20), and (d) I-AlSBA-15-(10).

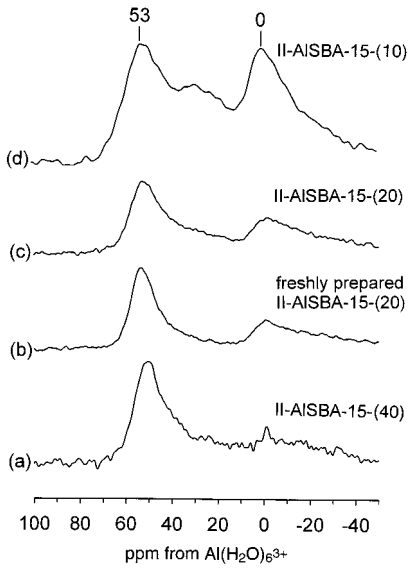

Figure 5. ^{27}Al MAS NMR spectra of calcined AlSBA-15 prepared by post synthesis of SBA-15 with aluminum isopropoxide in dry hexane: (a) II-AlSBA-15-(40), (b) freshly prepared II-AlSBA-15-(20), (c) II-AlSBA-15-(20), and (d) II-AlSBA-15-(10).

aluminum is covalently bound to four Si atoms via oxygen bridges. The chemical shift at 0 ppm can be assigned to octahedral aluminum (AlO_6 structural unit, Al(oct)).[8] The results clearly show the simultaneous presence of both AlO_4 and AlO_6 structural units. A comparison between spectrum b of a freshly prepared sample and spectrum c of the corresponding calcined sample shows that the line at 0 ppm decreases in intensity relative to the line at 53 ppm following calcination. This indicates that heat treatment enhances the incorporation of aluminum into the SBA-15 framework.

^{27}Al MAS NMR spectra of II-AlSBA-15 produced by reacting siliceous SBA-15 with aluminum isopropoxide in dry hexane (route 2), illustrated in Figure 5, also give two lines at 53 and 0 ppm. But in comparison with those

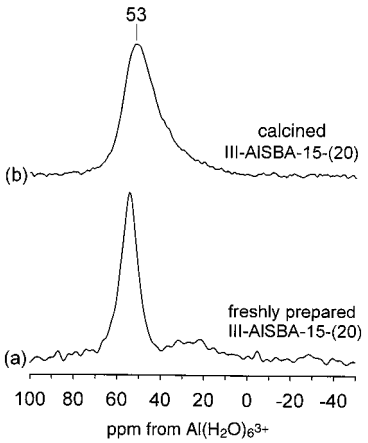

Figure 6. ^{27}Al MAS NMR spectra of AlSBA-15 prepared by postsynthesis of SBA-15 with sodium aluminate in aqueous solution: (a) Freshly prepared III-AlSBA-15-(20) and (b) III-AlSBA-15-(20) after calcination.

from I-AlSBA-15 (Figure 4) the 0 ppm line is broader and more intense. This indicates that a lower percentage of aluminum is incorporated into SBA-15 via this alumination procedure.

In contrast, the ^{27}Al MAS NMR spectra of III-AlSBA-15 produced by reacting siliceous SBA-15 with an aqueous solution of sodium aluminate (route 3), illustrated in Figure 6, exhibit only one resolved line at 53 ppm, corresponding to tetrahedral aluminum even for a freshly prepared sample. This result indicates that all aluminum has been incorporated into the siliceous framework of SBA-15.

The percentage of tetrahedral aluminum in each AlSBA-15 material can be calculated from the relative intensities of the 53 ppm line in the ^{27}Al MAS NMR spectra, assuming that the relative content of aluminum is proportional to the intensity of the ^{27}Al MAS NMR lines.[18] The results are presented as Al(tet)/(Al(tet)+Al(oct)) in Table 1.

ESR. ESR spectra of Cu(II) ion exchanged AlSBA-15 materials are illustrated in Figure 7. The spectra recorded at 77 K are well-resolved independent of the alumination procedure (Figure 7a−c) and show a single Cu(II) species described by $g_{||} = 2.392$, $g_{\perp} = 2.070$ and $A_{||} = 0.0149$ cm^{-1} with $A_{\perp}$ unresolved where A is the hyperfine coupling. The $g_{||}$ and $A_{||}$ parameters indicate an elongated octahedral Cu(II)−water complex[19,20] to which we assign this species. At 293 K, the Cu(II) ESR spectra become broader (Figure 7d) and appear to be overlapped by an isotropic Cu(II) species with $g = 2.156$. A broad isotropic ESR line of a fast tumbling $[Cu(H_2O)_6]^{2+}$ complex has been observed in different zeolites.[21] Thus, the observation of this broad isotropic ESR signal with $g = 2.156$ at 293 K is indicative of a rotating $[Cu(H_2O)_6]^{2+}$ complex.

The intensity of the ESR signal at 77 K based on double integration is more intense for III-AlSBA-15-(20) (Figure 7c), produced by reacting siliceous SBA-15 with an aqueous solution of sodium aluminate (route 3), than

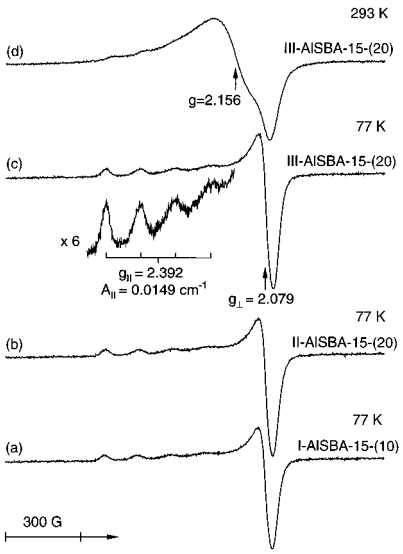

Figure 7. ESR spectra of Cu(II) ion-exchanged into (a) I-AlSBA-15-(10) at 77 K (b) II-AlSBA-15-(20) at 77 K, (c) III-AlSBA-15-(20) at 77 K, and (d) III-AlSBA-15-(20) at 293 K. The spectra are depicted on the same scale.

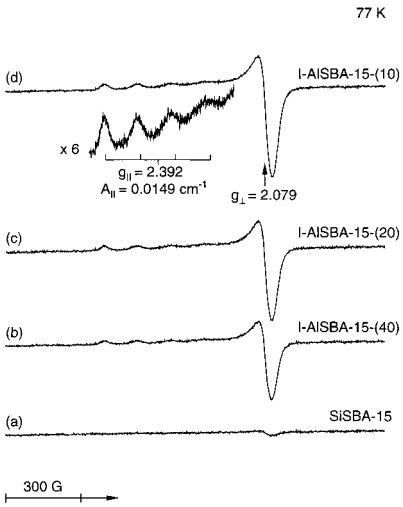

Figure 8. ESR spectra at 77 K of Cu(II) ion-exchanged into (a) siliceous SBA-15, (b) I-AlSBA-15-(40), (c) I-AlSBA-15-(20), and (d) I-AlSBA-15-(10). The spectra are depicted on the same scale.

for I-AlSBA-15-(10) and I-AlSBA-15-(20) (Figure 7a,b), produced via other routes; although the aluminum content in these latter cases is equal or higher than for I-AlSBA-15-(20) (Table 1).

To further evaluate the effect of alumination on the ion exchange capacity of SBA-15 and AlSBA-15, ESR spectra of a series Cu(II) ion exchanged AlSBA-15 materials with varying aluminum content are illustrated in Figure 8. Siliceous SBA-15 has essentially no ion-exchange capacity. All the Cu-AlSBA-15 materials exhibit the same Cu(II) species with $g_{||} = 2.392$, $g_{\perp} = 2.070$, and $A_{||} = 0.0149$ cm^{-1}. As expected, the Cu(II) ESR intensity increases linearly with increasing aluminum content.

Discussion

Pore Structure. Siliceous SBA-15 gives a XRD pattern of a hexagonal lattice with a $d(100)$ spacing of 105 Å (Figure 1), corresponding to a large unit cell

(18) Luan, Z.; Cheng, C.-F.; He, H.; Klinowski, J. *J. Phys. Chem.* **1995**, *99*, 10590.
(19) Pöppl, A.; Newhouse, M.; Kevan, L. *J. Phys. Chem.* **1995**, *99*, 10019.
(20) Hathaway, B. J.; Billing, D. E. *Coord. Chem. Rev.* **1970**, *5*, 143.
(21) Anderson, M. W.; Kevan, L. *J. Phys. Chem.* **1987**, *91*, 4174.

parameter a_0 = 122 Å ($a_0 = 2d(100)/\sqrt{3}$). The N_2 adsorption experiments reveal that this SBA-15 material possesses a narrow pore size distribution with an average pore size of about 62 Å and a high mesopore surface area A_{BJH} of 997 m^2/g (Table 2). This approximate pore size calculated by nitrogen physisorption is smaller than the repeat distance $d(100)$ spacing of 105 Å determined by XRD, because the latter includes the thickness of the pore wall. Thus, we can estimate that the pore walls of siliceous SBA-15 are ~43 Å thick consistent with the TEM observation. Such thicker silica walls are more thermally stable than the thinner walls (~12 Å) of siliceous MCM-41 materials[2,8] where significant unit cell expansion occurs following calcination.

Incorporation of aluminum into SBA-15 to produce AlSBA-15 by reacting SBA-15 with $AlCl_3$ in dry ethanol (route 1) does not much affect the original pore structure of the parent SBA-15. For I-AlSBA-15-(10) the observed specific surface area is still 874 m^2/g (Table 2). However, alumination by reacting SBA-15 with aluminum isopropoxide in dry hexane (route 2) or with an aqueous solution of sodium aluminate (route 3) significantly reduces the surface area and narrows the pore diameter of the parent SBA-15. For III-AlSBA-15-(20) the BET specific surface area is only 42% of the parent SBA-15 (Table 2). This indicates some modification of the tubular channels of SBA-15.

Aluminum Incorporation. Purely silicate materials have an electrically neutral framework and consequently no Brønsted acidity. When aluminum is incorporated into a silicate framework, it is expected that the aluminum adopts tetrahedral coordination to four silicon atoms via oxygen bridges and yields so-called structural hydroxyls which serve as Brønsted acid sites.[1,8] Aluminum that is not incorporated into the silicate framework is a nonframework species typically with octahedral coordination and does not contribute to the Brønsted acidity of these materials.[1] ^{27}Al MAS NMR spectroscopy seems to be the main technique for discriminating between tetrahedral framework and octahedral nonframework aluminum.[8] Although this is the typical interpretation, it should be noted that the NMR chemical shifts indicate the coordination, but not specifically whether the element is in the framework or not. For example, framework aluminum can coordinate to two additional ligands such as water and have distorted octahedral coordination.

Unfortunately, quantitative comparison of ^{27}Al MAS NMR spectra of alumiunum-containing silicates is somewhat limited, especially for thermally treated materials, due to significant second-order quadrupole interactions.[18] Thus, "NMR-invisible" aluminum has been discussed.[13,14] However, this obstacle can be largely overcome[18] by (1) using samples that are thoroughly hydrated, (2) using short radio frequency pulses, and (3) using rapid sample spinning. The ^{27}Al spectra reported in this work were measured under these conditions so a quantitative comparison is considered to be fairly reliable.

^{27}Al MAS NMR indicates that aluminum is incorporated into siliceous SBA-15, but with varying efficiency depending on the alumination procedure. By reacting SBA-15 with an aqueous solution of sodium aluminate (route 3), the resultant materials contain only tetrahedral aluminum which is likely in the framework (Table 1). In contrast, alumination by reaction with $AlCl_3$ in dry ethanol (route 1) or with aluminum isopropoxide in dry hexane (route 2) only achieves partial alumination as tetrahedral framework aluminum. It thus appears that the presence of Na^+ cations promotes the alumination process probably because Na^+ can balance the negative charge associated with tetrahedral framework aluminums.

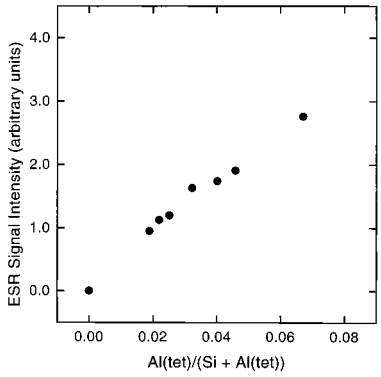

Figure 9. Dependence of Cu(II) ion exchange capacity of AlSBA-15 calculated from double integration of the ESR signal versus the framework Si/Al ratio from ^{27}Al MAS NMR (Table 1).

Like siliceous MCM-41 materials,[8,22] siliceous SBA-15 also possesses silanol groups on the wall surfaces. These silanol groups are suggested to serve as active sites for initial aluminum grafting as previously suggested for various metal ions grafted onto MCM-41 materials. To verify this assumption ^{29}Si MAS spectra have been collected for both siliceous SBA-15 and AlSBA-15 samples. They show one broad line attributable to $Si(OSi)_4$ units (Q^4 sites) (spectra not shown) and a shoulder attributed to $Si(OSi)_3OH$ units (Q^3 sites). This indicates the amorphous nature of the walls in SBA-15 as in MCM-41. Due to the poor resolution of the spectra, line deconvolution yielding Q^4/Q^3 ratios is ambiguous.

Ion Exchange. ESR spectra recorded at 77 K of Cu(II) ion exchanged AlSBA-15 exhibit a well-resolved axially symmetric Cu(II) signal assignable to isolated Cu(II)−water complexes (Figure 7). The ESR signal intensity depends not only on the aluminum content (Figure 8) but also on the alumination procedures. III-AlSBA-15 produced by reacting the SBA-15 with an aqueous solution of sodium aluminate (route 3) shows the highest Cu(II) ion exchange capacity in comparison with AlSBA-15 produced via route 1 and 2 alumination procedures with similar aluminum content (Figure 7). Since ^{27}Al MAS NMR shows that III-AlSBA-15 has a higher percentage of tetrahedral framework aluminum, this result indicates that the ion exchange capacity is associated with tetrahedral framework aluminum.

Cu(II) ion exchange capacities of AlSBA-15 produced via different alumination procedures and with variable Si/Al ratios are calculated by double integration of the ESR spectra and are plotted against the framework Si/Al ratio based on ^{27}Al MAS NMR (Table 1) in Figure 9. The Cu(II) ion exchange capacity of AlSBA-15 increases

(22) Kolodziejski, W.; Corma, A.; Navarro, M. T.; Pérez-Pariente, *J. Solid State NMR* **1993**, *2*, 253.

linearly with increasing tetrahedral framework aluminum content. Such a dependence of the transition metal ion exchange capacity on the aluminum content is common in crystalline zeolite materials.[23] Like zeolites and MCM-41[24] the ion exchange capacity of AlSBA-15 correlates well with the aluminum incorporated into the framework of SBA-15 materials.

In comparison with MCM-41 material where about 44% of the framework aluminums are accessible to effect Cu(II) ion exchange,[22] EPMA analysis of Cu(II) ion exchanged into AlSBA-15 shows that the Cu(II) ion exchange capacity corresponds to about 30% of the aluminums in the bulk and increases with increasing percentage of aluminum in the tetrahedral framework (Table 1). This suggests that some aluminums have penetrated into the SBA-15 silica walls during the alumination process and are not accessible for promotion of ion exchange. The amount of these seems slightly greater in SBA-15 compared to MCM-41. This difference is consistent with the thicker silica walls in SBA-15.

Conclusions

Mesoporous silica SBA-15 molecular sieve has been synthesized and incorporated with aluminum to produce AlSBA-15 via three postsynthesis procedures. Characterization shows that aluminum is mostly incorporated into silica SBA-15 in a range of Si/Al = 40−10. Alumination by reacting SBA-15 silica wall surfaces with $AlCl_3$ in dry ethanol (route 1) best maintain the original pore structure of the parent SBA-15, while alumination by reacting SBA-15 with aluminum isopropoxide in dry hexane (route 2) or with an aqueous solution of sodium aluminate (route 3) causes some structural disorder. However, the percentage of aluminum with tetrahedral symmetry in these materials is in the order route 3 > route 1 > route 2, indicating that aqueous alumination by sodium aluminate is most effective. The Cu(II) ion exchange capacity of AlSBA-15 is linearly dependent on the tetrahedral framework aluminum content. This suggests that the incorporated aluminum in the tetrahedral framework does serve as ion exchange sites.

Acknowledgment. This research was supported by the Robert A. Welch Foundation, the University of Houston Energy Laboratory and the National Science Foundation. M.H. wishes to thank Deutsche Forschungsgemeinschaft for support.

CM9900756

(23) Breck, D. W. *Zeolite Molecular Sieves*; Wiley-Interscience: New York, 1974.
(24) Luan, Z.; Xu, J.; Kevan, L. *Nukleonika* **1997**, *42*, 493.